SolarPACES 2022, 28th International Conference on Concentrating Solar Power and Chemical Energy Systems
Solar Industrial Process Heat and Thermal Desalination
https://doi.org/10.52825/solarpaces.v1i.745

Published: 10 Jan. 2024

# Dynamic Modeling of a Solar-to-Hydrogen Flexible High Temperature Steam Electrolysis Plant

Jake Immonen[1][https://orcid.org/0000-0003-4123-1625], and Kody M. Powell[1][https://orcid.org/0000-0001-9904-6671]

[1] University of Utah, USA

**Abstract.** Sustainble hydrogen production for use as a renewable combustible fuel and clean chemical feedstock is an important objective as the world moves towards a renewable energy future. High temperature steam electrolysis is a promising hydrogen production technology due to its reduced electric input that is offset by heat input into steam generation and steam superheating. An option to provide this heat is to use concentrating solar thermal technology that can sustainably provide heat input while renewable electricity is used for the electrolysis reaction. In this work, a solar-to-hydrogen high temperature steam electrolysis plant is designed and dynamically modeled, showing continuous hydrogen production by utilizing supplemental heating and efficient recuperative heating from the electrolysis product streams. Through this design, over 90% of the required heat input for the process can by met by a combination of solar and recuperative heat. Additionally, the plant can flexibility operate by ramping down hydrogen production and through flexible heat integration, which intelligently integrates solar heat based on solar conditions. Smooth operation with flexible hydrogen production is demonstrated which decreases electrical input during on-peak grid times and also decreases the total supplemental heat load over the course of a day from 26.1% to 24.5%. In addition, by using flexible heat integration, the plant can increase its solar heat usage by 4.1% relative to a base case. Both options for flexibility show efficient use of solar thermal energy to sustainably and continuously produce hydrogen.

**Keywords:** Solar Process Heat, Dynamic Modelling, Sustainable Hydrogen Production

## 1. Introduction

The production of hydrogen in a sustainable manner is becoming increasingly more relevant as the world looks for effective ways to produce renewable combustible fuels and renewably generated chemical feedstocks. Recent developments in solid oxide electrolysis cells (SOECs) have allowed for the potential of full-scale development of high temperature steam electrolysis (HTSE) which utilizes steam, typically at 800 ºC, to produce hydrogen and oxygen. The main benefits of HTSE include reduced electricity demand from offsetting heat input in steam generation and steam superheating, high electrolysis efficiencies, faster reaction kinetics, and the use of less expensive electrocatalysts [1]. Concentrating solar thermal (CST) technology can provide low cost heat to generate steam while renewable electricity can provide energy for electrolysis providing renewable hydrogen production. Some studies have shown dynamic solar operation to meet the heat input of HTSE [2], [3], but they did not effectively consider efficient dynamic operation of these plants needed to deal with the inherent variability of solar in realistic full-scale operation with reliable, continuous hydrogen production. Specifically, an operating scheme for a CST plant that works to maximize solar efficiency under different solar and production conditions has not been studied. In this work, a novel solar-to-hydrogen flexible high temperature steam electrolysis (SH-FHTSE) plant is designed and dynamically modeled,

demonstrating efficient operation under variable conditions while continuously and efficiently producing hydrogen.

The SH-FHTSE plant shows flexibility for two conditions. The first is flexible hydrogen production where the plant can ramp production up and down due to solar conditions or electricity pricing. The second is by utilizing flexible heat integration (FHI), which is a concept shown to increase solar utilization by lowering heat transfer fluid (HTF) collection temperatures and by flexibly delivering solar heat to different processes [4], [5]. The work outlines the modeling methods and dynamic results for constant and flexible hydrogen production as well as utilizing flexible heat integration built into the plant.

## 2. Methods

The SH-FHTSE plant design and modeling methods are outlined in the following sections. The designed plant is modeled in Simulink/MATLAB.

### 2.1. Plant Design

The SH-FHTSE plant is shown in Figure 1. The plant can be split into three sections: 1) parabolic trough collectors (PTCs) with thermal energy storage (TES), 2) anode and cathode stream heat exchanger trains, and 3) the electrolyzer.

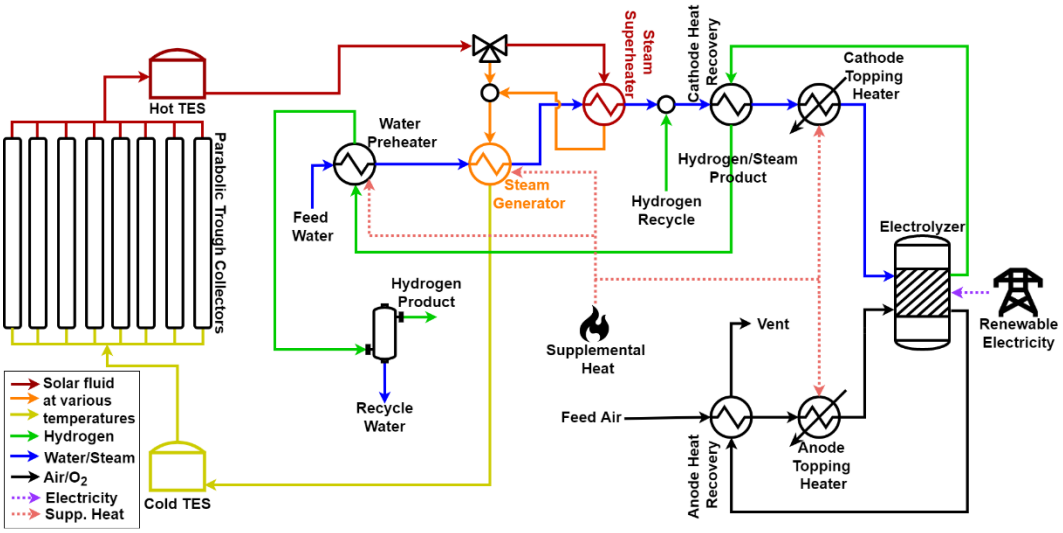


**Figure 1**. Flow diagram of the SH-FHTSE plant.

The PTCs provide renewable heat to the plant using CST, which heats up an HTF that exchanges heat with the cathode process stream before being reheated by the PTCs. This renewable heat reduces the required electrical load for the electrolysis process by 37% compared to a proton exchange membrane (PEM) electrolyzer which uses 55 kWh of electricity per kg of $H_2$ produced [6]. The anode and cathode heat exchanger trains use a combination of heat from the PTC HTF, heat recuperation from the electrolysis product streams, and supplemental heat to raise the anode and cathode stream temperatures to 800 ºC. The cathode stream is composed of water/steam at 1 atm. The water starts at 20 ºC and first has to have its temperature raised to the saturation temperature before entering a steam drum, which then fully evaporates the incoming water. A water preheater exchanges heat with the water and any excess heat required to raise the water to the saturation temperature is provided by a supplementary heater. The heat for the water preheater is lower quality recuperative heat and comes from the cathode product stream after it has exited the cathode recuperation heat exchanger. Saturated water then enters the steam drum, which is hybridized to be able to use solar thermal energy and supplemental heat so that the exiting steam mass flow rate matches the incoming

water. Following the steam drum is a solar steam superheater, which uses the high quality heat from the PTCs to superheat the water as much as possible. After the steam superheater, a small amount (10 mol%) of recycled hydrogen product is mixed into the cathode stream to avoid cathode oxidation in the electrolyzer. Following the steam superheater is the cathode recuperation heat exchanger, which exchanges the superheated steam with the electrolysis cathode product stream containing hydrogen and unreacted steam. A final supplementary heat exchanger, called the cathode topping heater ensures that the cathode stream has its temperature raised to 800 ºC before entering the electrolyzer.

The anode stream is composed of dry air at 1 atm. The air starts at 20 ºC and first goes into an anode recuperative heat exchanger, which raises the air temperature by exchanging the anode product stream with the incoming air. Next, a supplementary anode topping heater ensures that the air enters the electrolyzer at 800 ºC. The electrolyzer is made of stacks of SOECs which are composed of a three layer structure of porous cathode, an electrolyte, and a porous anode. Flow channels (for the anode stream and cathode stream) are located on either side of the three layer structure and enclosing the flow channels is interconnecting material that separates each cell. Electrical current flows from the cathode to the anode, providing energy for the electrolysis reaction, which produces hydrogen and oxygen from steam. The anode stream becomes oxygen-enriched air at the electrolyzer outlet, while the cathode stream becomes a gaseous mix of hydrogen and steam. Each product stream then goes into recuperative heat exchangers. Although not modeled, the cathode stream goes to a multi-stage compression and separation process where near pure hydrogen product is recovered and unreacted water knocked out by compression is recycled back into the start of the process. The oxygen-enriched air is vented to the environment.

The PTC part of the plant is designed based off of a previous work from Immonen et. al. [5]. The plant has a design direct normal irradiation (DNI) of 1000 W/m$^2$. The solar field can achieve 40.5 $MW_{th}$ at these conditions and the electrolysis solar process heating load is 21.8 $MW_{th}$, giving the plant a solar multiple of 1.86. The plant is equipped with hot and cold TES tanks with a capacity of 162 $MWh_{th}$. The electrolyzer is designed for an inlet flow of steam and air at 8 kg/s. The electrolyzer converts 72.5% of the incoming steam product, which corresponds to a thermoneutral potential with an average current density of 0.52 A/cm$^2$. With recycled hydrogen, this gives a hydrogen production rate of 55,680 kg/day.

## 2.2. Parabolic Trough Collector Plant Dynamic Model

The parabolic trough dynamic model is well detailed in [4], [5]. The PTC model is composed of three energy balances: one for the HTF, one for the absorber pipe, and one for the glass envelope. The PTC plant also contains sensible TES, where the HTF is stored in hot and cold TES tanks. The two tanks are modeled such that they are well-mixed and well-insulated.

## 2.3. Heat Exchanger Models

The anode and cathode recuperative heat exchangers, the water preheater, and steam superheater are all modeled as simplified versions of shell and tube counter-current heat exchangers. Energy balances for the fluid in the tubes ($TT$) and the fluid on the shell-side ($SS$) are represented by the following:

$$\frac{\partial}{\partial t}[T_i(x)] = \frac{\dot{m}_i}{\rho_i A_i^{HX}}\frac{\partial}{\partial x}[T_i(x)] - \frac{U^{HX} P_{tubes}}{\rho_i C_{p,i} A_i^{HX}}\left[T_i(x) - T_{j\neq i}(x)\right] \text{ for } i \in \{TT, SS\} \text{ and } j \in \{TT, SS\} \quad (1)$$

where $T$ is temperature, $x$ is the distance down the exchanger, $\dot{m}$ is mass flow rate, $\rho$ is density, $A^{HX}$ is the cross sectional area of flow, $U^{HX}$ is the overall heat transfer coefficient, $P_{tubes}$ is the total perimeter of the heat exchanger tubes, and $C_p$ is specific heat. The energy balance on the HTF through the steam drum is the same as Equation (1), but the overall heat transfer

coefficient is for only one moving fluid, the HTF, because the water is not moving in the steam drum. The rate of steam from solar heat is then given by:

$$\dot{m}_{steam} = \frac{\dot{m}_{HTF} C_{p,HTF} \Delta T_{HTF}}{\Delta H^{vap}} \quad (2)$$

where $\Delta H^{vap}$ is the enthalpy of vaporization of water. No dynamic models are created for the supplemental heating. The supplemental heaters for the preheater and steam generator raise the water to saturation and fully evaporate all of the water incoming to the steam drum. The cathode and anode topping heaters ensure that both streams enter the electrolyzer at 800 ºC. The supplemental heaters could be provided by electric heaters, but for cost efficiency purposes, natural gas fired heaters are likely for a 1st generation plant. In this work, for an emissions comparison to steam methane reforming, the most common method for hydrogen production currently, it is assumed that the supplemental heaters are natural gas with an 80% combustion efficiency. This translates to 247 kg $CO_2$ per $MWh_{th}$ of supplemental heat.

## 2.4. Electrolyzer Dynamic Model

The electrolyzer dynamic model follows that of [7] with one SOEC being modeled to represent the performance of thousands of cells which make up the electrolyzer. The dynamic model consists of four mass balances and four energy balances. The modeled cell is spatially varying as a function of $x$ down the length of the cell. The four mass balances for each species are shown below:

$$\frac{\partial}{\partial t}[C_i(x)] = -u_{C/A}\frac{\partial}{\partial x}[C_i(x)] + \frac{1}{h_{C/A}} v_i R(x), \text{ for } i \in \{H_2, H_2O, O_2, N_2\} \quad (3)$$

where $C$ is concentration, $u_{C/A}$ is the fluid velocity in the cathode or anode flow channel, $h_{C/A}$ is the height of the cathode or anode channel, $v$ is the stoichiometric coefficient of each reacting gas species, and $R$ is the rate of reaction. The rate of reaction depends on the local current density, $j(x)$, along the length of the cell:

$$R(x) = \frac{j(x)}{2F} \quad (4)$$

where $F$ is the Faraday constant. The four energy balances are separated for the cathode stream ($C$), anode stream ($A$), the porous cathode, anode and electrolyte lumped together as a unit called the electric conducting structure ($S$), and the interconnecting material between each cell ($I$). The energy balances on the cathode and anode stream are shown below:

$$\frac{\partial}{\partial t}[T_i(x)] = -u_i\frac{\partial}{\partial x}[T_i(x)] + \frac{k_i}{\rho_i C_{p,i} h_i}[T_S(x) - T_i(x)] + \frac{k_i}{\rho_i C_{p,i} h_i}[T_I(x) - T_i(x)] \text{ for } i \in \{C,A\} \quad (5)$$

where $k$ is the convective heat transfer coefficient of each stream. Next, an energy balance for the the electric conducting structure is:

$$\frac{\partial}{\partial t}[T_S(x)] = \frac{\lambda_S}{\rho_S C_{p,S}}\frac{\partial^2}{\partial x^2}[T_S(x)] - \frac{k_C}{\rho_S C_{p,S} h_S}[T_S(x) - T_C(x)] - \frac{k_A}{\rho_S C_{p,S} h_S}[T_S(x) - T_A(x)] - \frac{2}{\rho_S C_{p,S} h_S}\left[\frac{\sigma[T_S^4(x) - T_I^4(x)]}{\frac{1}{\epsilon_S}+\frac{1}{\epsilon_I}-1}\right] + \frac{1}{\rho_S C_{p,S} h_S}[-\Delta H^{rxn}(x)R(x) + j(x)U] \quad (6)$$

where $\lambda$, $\sigma$, $\epsilon$, $\Delta H^{rxn}$, and $U$ are the thermal conductivity, the Stefan-Boltzmann constant, the emissivity, the enthalpy of reaction, and the electric potential of the cell, respectively. Radiation is assumed to happen only between the two solids that are both flat plates parallel to each other. Lastly, the energy balance for the interconnecting material is:

$$\frac{\partial}{\partial t}[T_I(x)] = \frac{\lambda_I}{\rho_I C_{p,I}}\frac{\partial^2}{\partial x^2}[T_I(x)] - \frac{k_C}{\rho_I C_{p,I} h_I}[T_I(x) - T_C(x)] - \frac{k_A}{\rho_I C_{p,I} h_I}[T_I(x) - T_A(x)] + \frac{2}{\rho_I C_{p,I} h_I}\left[\frac{\sigma[T_S^4(x) - T_I^4(x)]}{\frac{1}{\epsilon_S}+\frac{1}{\epsilon_I}-1}\right] \quad (7)$$

The electric potential of the cell is assumed to be uniform along the length of the cell and is calculated based on the sum of reversible losses and irreversible losses in the cell including ohmic overpotential, cathode and anode concentration overpotentials, and cathode and anode activation overpotentials. The reversible potential is found via the Nernst equation and the ohmic overpotential is found via calculating the cell resistivity with conductivities and thicknesses of the porous cathode, anode, and electrolyte. The concentration overpotentials are functions of the various species concentrations and the effective diffusivity of oxygen from the cathode stream to the anode stream. The activation overpotentials are found via an extended form of the Butler-Volmer equation. All the irreversible losses are functions of the local current, so in order to find the electric potential, a system of equations must be solved which finds the local current $j(x)$ and electric potential, $U$, which satisfies the system of equations.

## 3. Results and Discussion

The plant is simulated to show how it can be flexible and effectively produce hydrogen using solar heat. First, constant plant operation is shown. Next, operation of the plant with flexible hydrogen production is demonstrated. Lastly, the plant is simulated using FHI showing how it can more efficiently utilize solar heat.

### 3.1. Constant Production Operation

To first demonstrate the SH-FHTSE plant, smooth, continuous operation is simulated. A day which has medium-high DNI throughout the day with some variability is chosen for this case with results shown in Figure 2.

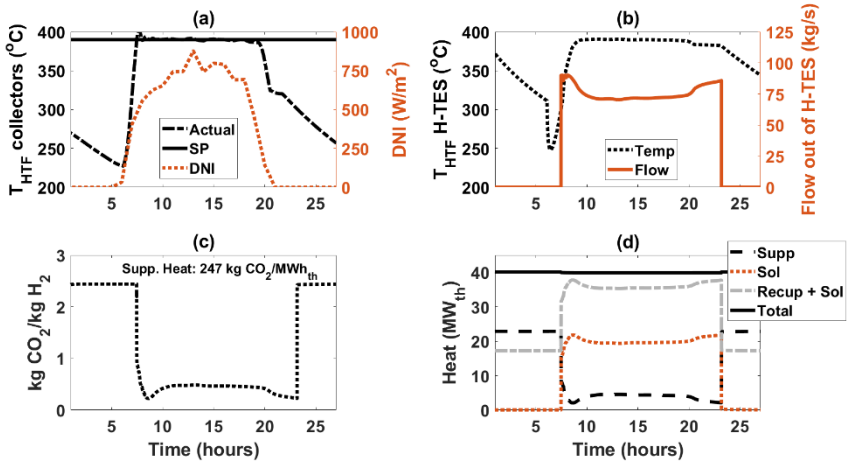


**Figure 2**. Constant hydrogen production results showing the DNI as well as the temperature and setpoint (SP) that the HTF is collected at (a), the flow and temperature of HTF from the hot-TES tank (b), the real-time $CO_2$ emissions from the process (assuming all the electric input is $CO_2$ free) (c), and the thermal heat breakdown provided to the process (d).

In the beginning of the day (starting at midnight), the plant is running and producing hydrogen with all of its heating load being met by supplemental heating. The electrolyzer is running in a thermoneutral operation producing a constant hydrogen production of 0.644 kg/s. The sun then begins to rise and HTF is collected at 390 ºC and immediately sent to the hot TES tank. Soon after the tank begins filling, hot HTF is then discharged from the tank to the steam superheater

and steam generator heat exchangers in series. The supplemental heating is then able to ramp down as solar heat takes its place. With solar heat superheating the steam, the cathode recuperative heat exchanger now exchanges less heat. This enables all of the water preheating to be fulfilled by the cathode product stream with no supplemental heating required in the water preheater. It also enables less supplemental heat to be used for the cathode topping heater. During this time of high quality heat discharge from the hot TES tank, 88-94% of the process heating load (including anode stream heating) is met by a combination of solar heat and recuperative heat. The hot TES tank discharges into the night until it empties when the process transfers back over to using all supplemental heat. This use of solar heat can be seen in the real-time $CO_2$ emissions plot where when solar heat is being used the $CO_2$ emissions are dropped drastically. During this entire time, the hydrogen production remains constant.

## 3.2. Flexible Production Operation

Flexible production of a HTSE plant could be beneficial to decrease hydrogen production during times without available solar energy to minimize supplemental heat usage or to reduce electric demand coming from the plant. Large industrial users often pay higher fees for energy usage and electric demand depending on the time of day. For example, for one electric rate schedule, this 'on-peak' time is from 3:00pm to 10:00pm on weekdays. Thus, if an electrolyzer plant wants to save on operating costs if may be beneficial for them to ramp down production and electric use during these on-peak times to avoid high operating costs. This type of operation is simulated for the same solar day as in the constant production operation. The operation of this day starts out the same as before and remains the same until 2:30pm when the electrolyzer plant then begins to ramp down production. The flow rates of the feed water and air are ramped down slowly, as modeled by a first order transfer function. During this time, the electrolyzer is also ramping down its electric input as it responds to the lower incoming flow. By 3:00pm, the electric input is reduced by 25% and the hydrogen production is 0.413 kg/s. Because the current is reduced to the electrolyzer, the individual cell voltage also drops below the thermoneutral cell potential, causing the temperature of the product streams out of the electrolyzer to drop to 750 ºC. As the flow rate of the water and air streams are ramped down, the HTF discharged from the hot TES tank is also ramped down to meet this lower heating demand. The solar heating continues to superheat steam and evaporate water during this lower production time until 10:00pm when the process ramps back up to its design levels. The HTF also ramps back up to meet this higher heat demand until the hot TES tank is empty. Because less total heat is required for this day the total supplemental heat decreases from to 26.1% to 24.5%. Figure 3 shows the heat load for this day as well as the electric load.

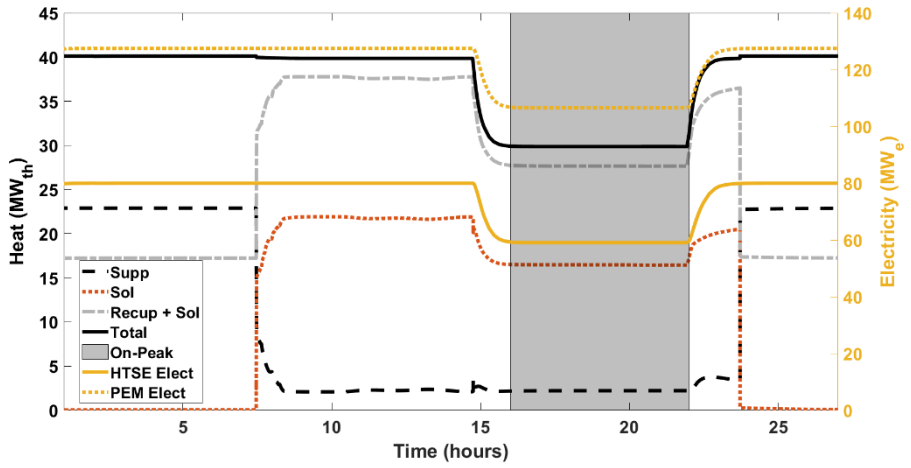


**Figure 3**. Flexible hydrogen production heat load and electric load. Electric load also shows an expected PEM electrolyzer electric load input for a comparison.

## 3.3. Flexible Heat Integration

The second option for flexibility in the plant is to use FHI, which is built into the plant in several ways. FHI allows for the HTF to be collected at lower temperatures for less than ideal solar conditions and also allows for heat to be delivered in a flexible way to the steam superheater and steam generator. A less than ideal solar day is chosen to demonstrate this operation. On this day, for the base case, the HTF collection setpoint is 390 ºC and the HTF is discharged to the steam superheater and steam generator in series. Since the solar conditions are poor, it is more beneficial to use FHI, where the HTF collection temperature setpoint is lowered to 365 ºC and the steam superheating solar heat exchanger is completely bypassed. In doing this, the HTF flow rate through the PTCs is increased due to the lower setpoint. This reduces radiative losses in the field and increases the amount of solar energy transferred to the process. Using FHI on this day increases the solar heat delivered to the process by 4.1% relative to the base case operation. Figure 4 shows the PTC temperature collection and heat load breakdown.

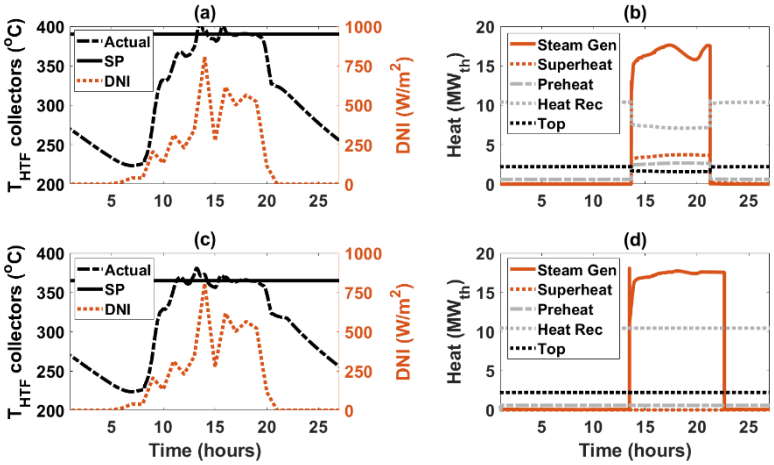


**Figure 4**. Results demonstrating operation without ((a) and (b)) and with ((c) and (d)) FHI.

## 3.4. Results Summary

The results of the four different days of operation are summarized in Table 1. The constant production process day is able to exchange more solar heat than the flexible production day due to not having a step change in the process, but it has a higher average emission rate and total supplemental heat share because more total heat energy is required. Both conditions only need around 25% of the total heat supplied for the day to be from a supplemental source. Using FHI increases the solar use by 6 $MWh_{th}$. which in turn decreases the average emissions. Even on this poor solar day, only 40% of the total heat load needs to be supplied by supplementary sources. For all of the days simulated, the average emission rate (assuming all $CO_2$ free electricity for the electrolysis reaction) is well below 9.01 kg $CO_2$/kg $H_2$, an average found at steam methane reforming plants in the U.S. [8].

**Table 1.** Results summary for the two days and four conditions simulated.

| Operation Type | Solar Heat ($MWh_{th}$) | Avg. Emission Rate (kg $CO_2$/kg $H_2$) | Total Supplemental Heat Share (%) |
|---|---|---|---|
| Constant Production | 314.2 | 1.102 | 26.1 |
| Flexible Production | 308.9 | 0.977 | 24.5 |
| Base FHI | 145.6 | 1.787 | 41.9 |
| FHI | 151.6 | 1.737 | 40.6 |

# 4. Conclusions

In this study, a novel solar-to-hydrogen high temperature steam electrolysis plant is dynamically modeled. The plant shows continuous hydrogen production with instances of over 90% of the total heat input to the plant being supplied by a combination of solar and recuperative heat. The plant demonstrates smooth operation for flexible hydrogen production that responds to peak demand pricing from the electric grid. This enables less supplemental heat to be used while also potentially saving on utility costs. The plant also utilizes flexible heat integration, which enables up to 4.1% more solar energy going to process heat. Overall, this work demonstrates flexible ways to efficiently produce hydrogen from CST with realistic dynamic scenarios.

## Data availability statement

TMY3 weather data for Salt Lake City, UT can be accessed via the NSRDB [9].

## Underlying and related material

Supplementary model details can be found on GitHub [10].

## Author contributions

Jake Immonen: Conceptualization, Methods, Software, Validation, Formal analysis, Investigation, Data curation, Writing – original draft, Writing – review & editing, Visualization. Kody M. Powell: Conceptualization, Methods, Writing – review & editing, Visualization, Supervision, Project administration, Funding acquisition.

## Competing interests

The authors declare no competing interests.

## Funding

This work is funded by the United States Department of Energy (DOE) under the DE-EE0009708 grant, which is affiliated with the DOE Industrial Assessment Centers Program.

## References

1. S. Alia, D. Ding, A. McDaniel, F. M. Toma, and H. N. Dinh, “Chalkboard 2 - How to Make Clean Hydrogen,” Electrochem. Soc. Interface, vol. 30, no. 4, pp. 49–56, Jan. 2021, doi: https://doi.org/10.1149/2.f13214if.
2. A. Houaijia, M. Roeb, N. Monnerie, and C. Sattler, “Solar power tower as heat and electricity source for a solid oxide electrolyzer: a case study,” Int. J. Energy Res., vol. 39, no. 8, pp. 1120–1130, Mar. 2015, doi: https://doi.org/10.1002/er.3316.
3. S. Koumi Ngoh, L. M. Ayina Ohandja, A. Kemajou, and L. Monkam, “Design and simulation of hybrid solar high-temperature hydrogen production system using both solar photovoltaic and thermal energy,” Sustain. Energy Technol. Assessments, vol. 7, pp. 279–293, Sep. 2014, doi: https://doi.org/10.1016/j.seta.2014.05.002.
4. J. Immonen, K. Mohammadi, and K. M. Powell, “Simulating a solar parabolic trough collector plant used for industrial process heat using an optimized operating scheme that utilizes flexible heat integration,” Sol. Energy, vol. 236, pp. 756–771, Apr. 2022, doi: https://doi.org/10.1016/j.solener.2022.03.044.
5. J. Immonen and K. M. Powell, “Dynamic optimization with flexible heat integration of a

solar parabolic trough collector plant with thermal energy storage used for industrial process heat," Energy Convers. Manag., vol. 267, Sep. 2022, doi: https://doi.org/10.1016/j.enconman.2022.115921.
6. IRENA, "Green Hydrogen Cost Reduction: Scaling up Electrolysers to Meet the 1.5°C Climate Goal," Abu Dhabi, 2020.
7. Q. Cai, N. P. Brandon, and C. S. Adjiman, "Modelling the dynamic response of a solid oxide steam electrolyser to transient inputs during renewable hydrogen production," Front. Energy Power Eng. China, vol. 4, no. 2, pp. 211–222, May 2010, doi: https://doi.org/10.1007/s11708-010-0037-6.
8. P. Sun et al., "Criteria Air Pollutants and Greenhouse Gas Emissions from Hydrogen Production in U.S. Steam Methane Reforming Facilities," Environ. Sci. Technol., vol. 53, no. 12, pp. 7103–7113, Apr. 2019, doi: https://doi.org/10.1021/acs.est.8b06197
9. "NSRDB: National Solar Radiation Database," National Renewable Energy Laboratory. https://nsrdb.nrel.gov/ (accessed May 20, 2022).
10. J.Immonen,"SolarPACES2022_SuppInfo." https://github.com/jimmonen11/SolarPACES2022_SuppInfo.